JACS
JOURNAL OF THE AMERICAN CHEMICAL SOCIETY
Article
pubs.acs.org/JACS

Reversible Interconversion Between a Monomeric Iridium Hydroxo and a Dinuclear Iridium μ-Oxo Complex

Richard J. Burford,[†] Warren E. Piers,*[,†] Daniel H. Ess,[‡] and Masood Parvez[†]

[†]Department of Chemistry, University of Calgary, 2500 University Drive NW, Calgary, Alberta, Canada T2N 1N4,
[‡]Department of Chemistry and Biochemistry, Brigham Young University, Provo, Utah 84602, United States

Supporting Information

ABSTRACT: Treatment of the ($PC_{sp^2}P$)$Ir^{I}Cl$ complexes $\mathbf{2}^{\mathbf{R}}$ (R = ^{i}Pr, ^{t}Bu) with cesium hydroxide in THF leads to the corresponding monomeric Ir(I) hydroxo complexes $\mathbf{5}^{\mathbf{R}}$ in good to excellent yields of 70% (R = ^{i}Pr) and 92% (R = ^{t}Bu). The compounds are green in color and while they exhibit very similar ^{31}P NMR data to the chlorides **2**, the ^{1}H NMR spectrum of each features a triplet ($^{3}J_{HP}$ = 3.8 Hz) at 4.22 (R = ^{t}Bu) and 4.31 (R = ^{i}Pr) ppm that broadens in the presence of excess water and exchanges deuterium with D_2O. Bands at 3642 and 3625 cm^{-1} are observed in the IR spectrum for the ν_{OH} stretch. In the case of R = ^{i}Pr, a second product is observed in the crude reaction mixture and dominates when $\mathbf{5}^{\mathbf{^{i}Pr}}$ is heated under vacuum and H_2O is removed. This product is deep blue in color, and an X-ray crystal structure analysis reveals it to be the S_4 symmetric dinuclear ($PC_{sp^2}P$)Ir−O−Ir($PC_{sp^2}P$) complex $\mathbf{6}^{\mathbf{^{i}Pr}}$, which features a μ-oxo ligand along an allene-like molecular core. Time-dependent DFT calculations with the M06 density functional show that a metal-to-ligand HOMO−LUMO excitation is mainly responsible for the blue color. Upon reaction of $\mathbf{6}^{\mathbf{^{i}Pr}}$ with water, monomeric hydroxo complex $\mathbf{5}^{\mathbf{^{i}Pr}}$ is quantitatively regenerated. Further, reaction of $\mathbf{6}^{\mathbf{^{i}Pr}}$ with an excess of phenol smoothly yields the previously prepared ($PC_{sp^2}P$)IrOPh complex $\mathbf{3}^{\mathbf{^{i}Pr}}$. Kinetic studies of the reaction indicated that it is first order in both [$\mathbf{6}^{\mathbf{^{i}Pr}}$] and [HOPh] and exhibits a k_H/k_D of 1.9 when DOPh is employed. Eyring analysis is consistent with the bimolecular nature of the reaction, with $\Delta H^{\ddagger}$ = 13.1(5) kcal mol^{-1} and $\Delta S^{\ddagger}$ = −13(2) cal K^{-1}. Finally, k_{obs} is observed to increase when electron-withdrawing groups are incorporated in the *para* position of the phenol substrate and decrease when electron-donating groups are employed. These observations suggest that the rate-limiting step in this reaction is protonation of the μ-oxo ligand by the phenol substrate. This reaction serves as a model system for the reversible condensation of metal hydroxo ligands to form metal oxo moieties.

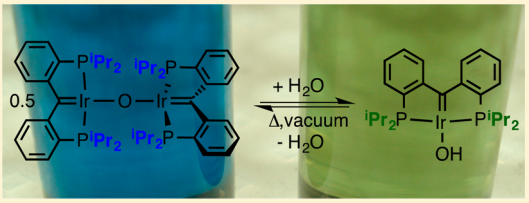

INTRODUCTION

One of the primary tenets of homogeneous catalysis is that intimate knowledge of the mechanisms by which a catalyst operates is critical to improving a catalyst's performance through rational modification. There is a large body of accumulated mechanistic knowledge concerning the transformations of hydrocarbyl ligands at transition metal centers[1] and this foundation of fundamental research has resulted in many economically important catalytic processes.[2−4] However, with the exception of proton coupled electron transfer processes,[5,6] there is less knowledge about how archetypical ligands based on oxygen are transformed within a transition metal's coordination sphere in similar ways by which hydrocarbyl ligands are manipulated.[7−9] Such transformations are likely to be important in catalytic water splitting schemes,[10,11] and as society moves toward carbon-free energy sources, basic knowledge concerning these fundamental transformations will be required.

There have been several reports detailing the effectiveness of organometallic complexes of iridium[12−18] as precatalysts for the water splitting reaction.[19] Some concerns have been raised that the role of these molecular species is essentially to deposit nanoparticulate iridium oxide,[20] which is also an active water oxidation catalyst, but it has been conclusively demonstrated[21] that homogeneous catalytic pathways mediated by organometallic species are viable when oxidatively stable supporting ligands are employed.[22] While the homogeneity of these reactions has been convincingly established, the harshness of the reaction conditions and the paramagnetism of some intermediates make it difficult to experimentally establish the structural properties of the species involved along the catalytic pathway,[23−25] let alone the intimate mechanistic details concerning their interconversion.

We,[26] and others,[27−36] have become interested in establishing the basic mechanistic precepts of such transformations. Our approach[37] has been to use the principles of ligand design to conceive molecular platforms which will support well-defined complexes of archetypical oxygen-based ligands (for example, H_2O, HO^-, O^{2-}, HO_2^-) and identify reactions in which they are interconverted; mechanistic studies on amenable systems will provide basic information concerning these important processes. Recently, we described iridium(I) derivatives of a novel tridentate "pincer" ligand framework in which the anchoring central ligating point is a strongly donating diarylcarbene moiety and the flanking donor arms are aryl dialkyl phosphines.[38]

Received: December 12, 2013
Published: February 5, 2014

   dx.doi.org/10.1021/ja412650s | J. Am. Chem. Soc. 2014, 136, 3256−3263

The aryl linking groups[39,40] prevent β elimination side reactions[41] that occur in the fully saturated analog,[42,43] while the dialkylphosphine arms provide more electron-rich donors than diaryl groups.[44,45] The $PC_{sp^2}P$ iridium(I) chloride complexes $\mathbf{2}^{\mathbf{R}}$ (R = ^{i}Pr, ^{t}Bu) were prepared via reversible elimination of H_2 from the Ir(III) $PC_{sp^3}P$ hydrido chlorides $\mathbf{1}^{\mathbf{R}}$. The chloride ligands in $\mathbf{2}^{\mathbf{R}}$ could be functionalized to phenoxy ($\mathbf{3}^{\mathbf{R}}$) derivatives via salt metathesis with NaOPh (Scheme 1). Formal addition of

Scheme 1

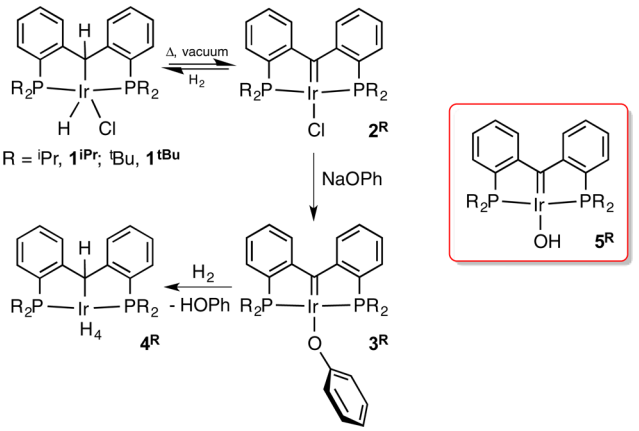

H_2 across the Ir=C bonds in $\mathbf{3}^{\mathbf{R}}$ is also facile but yields the $PC_{sp^3}P$ iridium polyhydrides[46] $\mathbf{4}^{\mathbf{R}}$ and phenol presumably via reductive elimination from phenoxy hydride intermediates related to compounds $\mathbf{1}^{\mathbf{R}}$. These transformations illustrate the ability of the $PC_{sp^2}P$ ligand to be involved in hydrogen atom management and motivated us to target the $(PC_{sp^2}P)$IrOH derivatives $\mathbf{5}^{\mathbf{R}}$ with a view to studying their reactivity; we describe these efforts herein.

RESULTS AND DISCUSSION

Synthesis and Characterization. Conversion of the iridium(I) carbene chlorides $\mathbf{2}^{\mathbf{R}}$ to the corresponding hydroxides is best accomplished by treatment with cesium hydroxide[47] in wet THF (Scheme 2). Other sources of hydroxide (NaOH,

Scheme 2

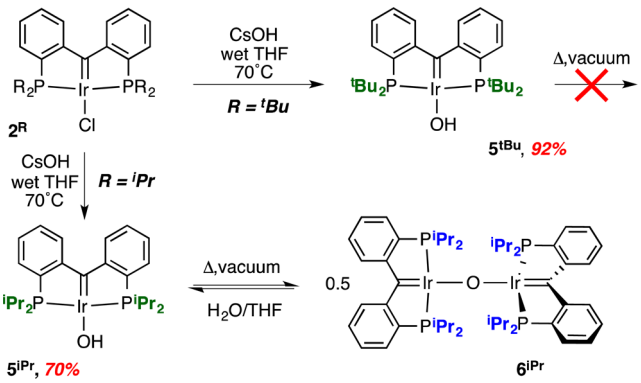

KOH,[48] Ph_3SnOH, Ag_2O/H_2O[49]), some proven to work well for iridium chlorides, were less effective. For $\mathbf{2}^{\mathbf{tBu}}$, the reaction with $CsOH/H_2O$ proceeds smoothly at 70 °C over the course of several hours, although there is little color change apparent, and the ^{31}P NMR chemical shift of 58.0 ppm is essentially the same as that found for the chloride starting material.[38] Nevertheless, workup lead to isolation of a green crystalline powder whose ^{1}H NMR spectrum displayed subtle differences to that obtained for $\mathbf{2}^{\mathbf{tBu}}$ and also exhibited a diagnostic triplet ($^{3}J_{HP}$ = 3.8 Hz) at 4.22 ppm, integrating to one hydrogen. This is significantly upfield of the resonances observed at 7.9−8.3 ppm for related terminal hydroxo Ir(I) complexes supported by pyridyl diimine pincer ligands.[50] This signal broadened in the presence of added H_2O and disappeared when D_2O was added to solutions of $\mathbf{5}^{\mathbf{tBu}}$. A signal at 202.7 ppm in the ^{13}C NMR spectrum is slightly downfield of that observed for the carbene carbon in $\mathbf{2}^{\mathbf{tBu}}$ (197.5 ppm)[38] but indicates retention of the diarylcarbene moiety. In the IR spectrum (Figure S1), a band at 3642 cm^{-1} was assigned to the ν_{O-H} stretching frequency; this band appeared at 2688 cm^{-1} in d_1-$\mathbf{5}^{\mathbf{tBu}}$.[51] Finally, a peak at m/z = 664.2554 in the high-resolution mass spectrum matches the calculated mass of $\mathbf{5}^{\mathbf{tBu}}$ (664.2575). Taken together, these data confirm the formation of the monomeric terminal hydroxo iridium(I) complex $\mathbf{5}^{\mathbf{tBu}}$. While several monomeric Ir(III) hydroxo compounds have been reported,[34,35,47,52−56] Ir(I) examples are more rare[48,50,57−59] and have a tendency to exist as dimers[58,59] unless sterically bulky ligands are employed.

In the case of the sterically more open $\mathbf{2}^{\mathbf{iPr}}$, the reaction with $CsOH/H_2O$ was less straightforward. When monitored by *in situ* NMR spectroscopy, again the ^{31}P NMR resonance exhibited little change from that observed for the chloro complex $\mathbf{2}^{\mathbf{iPr}}$, but in the ^{1}H NMR spectrum, a triplet at 4.31 ppm ($^{3}J_{HP}$ = 3.8 Hz) indicated the presence of an Ir−OH moiety and formation of $\mathbf{5}^{\mathbf{iPr}}$. A signal for the carbene carbon at 204.8 ppm in the ^{13}C NMR spectrum was also consistent with successful metathesis. An IR spectrum of this solution exhibited a band at 3625 cm^{-1} that shifted to 2685 cm^{-1} in the analogous d_1-$\mathbf{5}^{\mathbf{iPr}}$. However, attempts to work up this reaction by removal of the solvent *in vacuo* resulted in a color change of the solution from forest green to a deep blue color. Multinuclear NMR spectroscopic analysis of the residue indicated the presence of a new species along with $\mathbf{5}^{\mathbf{iPr}}$, with a resonance in the ^{31}P NMR spectrum at 38.0 ppm. After exposing the reaction residue to dynamic vacuum for 12 h at 70−80 °C, this species was the sole constituent of the product mixture. A signal at 185.1 ppm in the ^{13}C NMR spectrum indicated retention of the diarylcarbene moiety, but in the ^{1}H NMR spectrum the absence of a one-proton triplet suggested that the hydroxo ligand was absent in this blue species. Significantly, addition of degassed water to a THF solution of this compound instantaneously gave a blue to green color change and regenerated the spectrum of $\mathbf{5}^{\mathbf{iPr}}$; pure samples of this compound could be isolated from this medium. Furthermore, addition of activated molecular sieves to green solutions of $\mathbf{5}^{\mathbf{iPr}}$ resulted in the appearance of the blue color of the second species.

The nature of the blue species was confirmed by X-ray crystallography on blue crystals with a hexagonal habit grown from THF/toluene solutions (1:1) at −30 °C. The structure is depicted in Figure 1, along with selected metrical data and shows $\mathbf{6}^{\mathbf{iPr}}$ to be a dinuclear μ-oxo complex with allene-like structure in which the ruffling of the aryl groups in the orthogonal $PC_{sp^2}P$ ligand atoms results in S_4 symmetry. The atoms along the C(1)−Ir(1)−O(1)−Ir(1)′−C(1)′ vector are related by symmetry, and the angles C(1)−Ir(1)−O(1) and Ir(1)−O(1)−Ir(1)′ are 180.0°. The C(1)−Ir(1) distance of 1.936(5)Å is comparable to the values of observed for related $(PC_{sp^2}P)$Ir−X compounds we have reported (X = Cl,[38] 1.899(7)Å; 2,4,6-$(CH_3)_3C_6H_2$ (Mes),[38] 1.947(4)Å; N=C(CH_3)−,[60] 1.932(6)Å). The

dx.doi.org/10.1021/ja412650s | J. Am. Chem. Soc. 2014, 136, 3256−3263

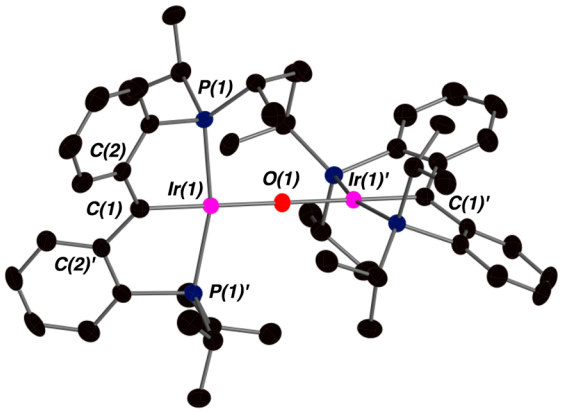

Figure 1. Thermal ellipsoid diagram (50%) of $\mathbf{6}^{i\mathrm{Pr}}$. Selected bond distances (Å): Ir(1)−C(1), 1.936(5); Ir(1)−P(1), 2.2982(9); Ir(1)−O(1), 1.9432(2). Selected bond angles (°): C(1)−Ir(1)−O(1), 180.0; Ir(1)−O(1)−Ir(1)′, 180.0; P(1)−Ir(1)−P(1)′, 163.67(5); C(2)−C(1)−C(2)′, 118.2(5).

Ir(1)−O(1) bond length of 1.9432(2)Å is similar to that of 1.9142(1)Å found for the Ir(IV)−Ir(IV) dinuclear species $Mes_3Ir{-}O{-}IrMes_3$ reported by Brown et al.,[61] despite its distinct difference in geometry and formal oxidation state from $\mathbf{6}^{i\mathrm{Pr}}$. The dinuclear μ-oxo species $\mathbf{6}^{i\mathrm{Pr}}$ is therefore notable since oxo ligands are typically associated with higher oxidation-state metal complexes. Since there is no evidence that compound $\mathbf{5}^{t\mathrm{Bu}}$ undergoes a similar condensation to form "$\mathbf{6}^{t\mathrm{Bu}}$", the formation of $\mathbf{6}^{i\mathrm{Pr}}$ is allowed by the slightly lower steric demands of the $P(^i\mathrm{Pr})_2$ groups.

The deep blue color of $\mathbf{6}^{i\mathrm{Pr}}$ is striking in light of Crabtree's extensive investigations into the nature of the so-called "blue layer" observed to form in many iridium-based water oxidation catalyst systems.[22] TEM-EDX analyses of samples of $\mathbf{6}^{i\mathrm{Pr}}$ prepared from dry THF solutions showed only evidence of >10 μm sized amorphous particles with the appropriate elemental composition and no evidence for formation of nanoparticulate IrO_2 (Figure S2). We conclude that the blue color of solutions of $\mathbf{6}^{i\mathrm{Pr}}$ is due to the compound itself and not iridium oxide nanoparticles. In the Crabtree studies on *bona fide* homogeneous systems of blue color, the blue compound was assigned as a dicationic Ir(IV)−Ir−(IV) dimer with two bent μ-oxo ligands;[22] absorptions at 590−608 nm with absorptivities of $\varepsilon \approx 1800\ M^{-1}\ cm^{-1}$ in the UV−vis spectrum were observed, the λ_{max} depending on the nature of the supporting bidentate ligand present. Dinuclear $\mathbf{6}^{i\mathrm{Pr}}$ exhibits a similar absorption at 608 nm ($\varepsilon = 3120\ M^{-1}\ cm^{-1}$ in THF), a feature that is completely absent from solutions of the *bona fide* mononuclear hydroxo complex $\mathbf{5}^{t\mathrm{Bu}}$. This absorption thus appears to be associated with the C═Ir−O−Ir═C molecular core; to gain further insight into this transition, we performed DFT and TD-DFT computations on $\mathbf{6}^{i\mathrm{Pr}}$.

Ground-state and TD-DFT calculations were carried out in Gaussian 09[62] with the M06[63,64] density functional and 6-31G(d,p)[LANL2DZ] basis set. The optimized geometry of $\mathbf{6}^{i\mathrm{Pr}}$ is structurally very similar to the X-ray structure shown in Figure 1. For example, the calculated Ir−C1 (Ir−carbene) bond length is 1.932 Å, which is very close to the 1.936(5) Å experimental bond length. Additionally, the calculated Ir−O and Ir−P bond lengths are 1.974 and 2.331 Å, respectively. These bond lengths also compare very well to the experimental bond lengths of 1.9432(2) and 2.2982(9) Å.

TD-DFT calculations reveal that there is a major and minor excitation associated with the $\mathbf{6}^{i\mathrm{Pr}}$ complex (Figure S3). The major excitation, which is responsible for the blue color of the $\mathbf{6}^{i\mathrm{Pr}}$ complex, occurs at 586 nm with an oscillator strength of 0.7089. A minor excitation was also calculated at 399 nm with an oscillator strength of 0.1152. Inspection of the orbital transitions responsible for the calculated 586 nm excitation reveals that it is a pair of degenerate HOMO−LUMO excitations. One of these degenerate pairs is shown in Figure 2 as a 237 → 238 transition.

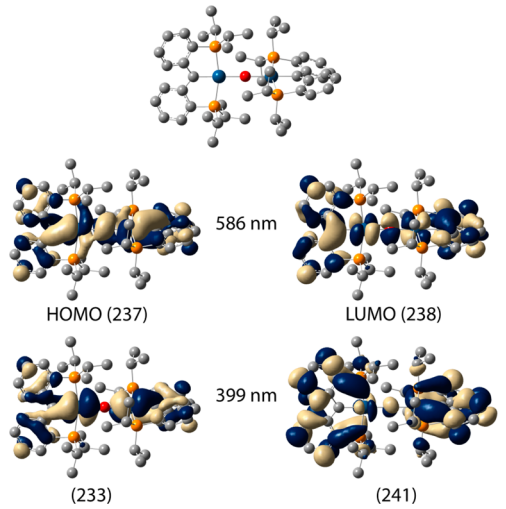

Figure 2. Occupied and unoccupied orbitals responsible for the dominant excitations of $\mathbf{6}^{i\mathrm{Pr}}$.

The HOMO orbital is mainly metal based and extends across the Ir−O−Ir bridge as an antibonding $Ir(d_\pi)-O(p_\pi)-(d_\pi)$ combination. The LUMO orbital is mainly ligand based and has a significant contribution from the carbene C1 atom that is directly bonded to the Ir metal center. This HOMO−LUMO excitation responsible for the blue color of the $\mathbf{6}^{i\mathrm{Pr}}$ is different than the excitation proposed to be responsible for the Crabtree blue dimer, where the major transitions arise from excitation of Ir(IV) centered electrons into Ir═O $d_\pi-p_\pi^*$ orbitals.[22] Given the differing formal oxidation states characterizing these two compounds, the distinct character of the transitions giving rise to the blue color is perhaps not too surprising. The minor excitation for $\mathbf{6}^{i\mathrm{Pr}}$ calculated to be at 399 nm is due to occupied to unoccupied orbital transitions 233 → 241 and 237 → 240. Orbital 233 is a nonbonding $Ir(d_\pi)-O(p_\pi)-(d_\pi)$ combination with no contribution from the $O(p_\pi)$ orbital. Unoccupied orbitals 240 and 241 are PCP ligand based with very little contribution from the carbene C1 atom, which is likely the origin of the decreased intensity.

Kinetic Studies. As shown in Scheme 1, the reaction of $\mathbf{6}^{i\mathrm{Pr}}$ with water rapidly regenerates the hydroxo complex $\mathbf{5}^{i\mathrm{Pr}}$. As such, this system offers an opportunity to study the mechanism of reversible interconversion between two hydroxo ligands and a μ-oxo group. Given the facility of the reaction of $\mathbf{6}^{i\mathrm{Pr}}$ with water and the ready availability of pure samples of the dinuclear blue oxo species, we chose to probe the process from this direction. By the principle of microscopic reversibility,[65] this would also provide information on the forward condensation reaction.

First, we sought to firmly establish the nuclearity of $\mathbf{5}^{i\mathrm{Pr}}$ in solution and the solid state, since it is conceivable that it could exist as a dimer with μ-hydroxo bridges. Despite many attempts, we were unable to grow suitable crystals for X-ray analysis of this

dx.doi.org/10.1021/ja412650s | J. Am. Chem. Soc. 2014, 136, 3256−3263

compound or its *tert*-butyl congener. EI-MS analysis of solutions of $\mathbf{5}^{i\mathrm{Pr}}$ gave the expected m/z of 608.1924, but more convincing evidence of its mononuclearity came from DOSY NMR experiments in which it was benchmarked against the demonstrably mononuclear chloride $\mathbf{2}^{i\mathrm{Pr}}$ and dinuclear $\mathbf{6}^{i\mathrm{Pr}}$ (see Table S1 and Figure S4). These experiments yielded estimates of the molecular volume for $\mathbf{2}^{i\mathrm{Pr}}$ (32 nm^3), $\mathbf{5}^{i\mathrm{Pr}}$ (36 nm^3), and dinuclear $\mathbf{6}^{i\mathrm{Pr}}$ (91 nm^3), clearly suggesting that the hydroxo complex exists as a mononuclear species in solution.

With this in mind, we attempted to follow the reaction of $\mathbf{6}^{i\mathrm{Pr}}$ with H_2O in THF solution at low temperature. Unfortunately, no reaction occurred below 253 K, possibly due to the formation of insoluble THF-hydrate clathrates.[66,67] Furthermore, once the sample reached temperatures above this threshold, reaction to form 2 equiv of hydroxo product $\mathbf{5}^{i\mathrm{Pr}}$ was essentially instantaneous and extracting kinetic data by NMR spectroscopy was not possible in this solvent. Use of other solvents with which $\mathbf{6}^{i\mathrm{Pr}}$ is compatible lead to similar difficulties, precluding kinetic analysis of this reaction by these methods.

Because of these technical challenges, we sought a suitable surrogate substrate for H_2O for examination of the activation of an O–H bond at the Ir–O–Ir core of $\mathbf{6}^{i\mathrm{Pr}}$. Small aliphatic alcohols like methanol or ethanol, which are closest to water in terms of pK_a values, were not suitable due to the facile decarbonylation[68−71] of the (PC$_{sp^2}$P)Ir(OR) complexes formed upon reaction of $\mathbf{6}^{i\mathrm{Pr}}$ with ROH.[72] Bulkier *tert*-butanol, with no β hydrogens, required higher temperatures (>80 °C) to react with $\mathbf{6}^{i\mathrm{Pr}}$ and produced mainly $\mathbf{5}^{i\mathrm{Pr}}$ via isobutene elimination.[47] Therefore, although significantly more acidic than H_2O (pK_a = 15.7), we chose phenol (pK_a = 9.95) as a model substrate for examining the reactivity of $\mathbf{6}^{i\mathrm{Pr}}$ with OH bonds.

As shown in Scheme 3, the product of reaction of $\mathbf{6}^{i\mathrm{Pr}}$ with an excess of phenol is the known complex[38] $\mathbf{3_H}^{i\mathrm{Pr}}$ (X = H). Similar

Scheme 3

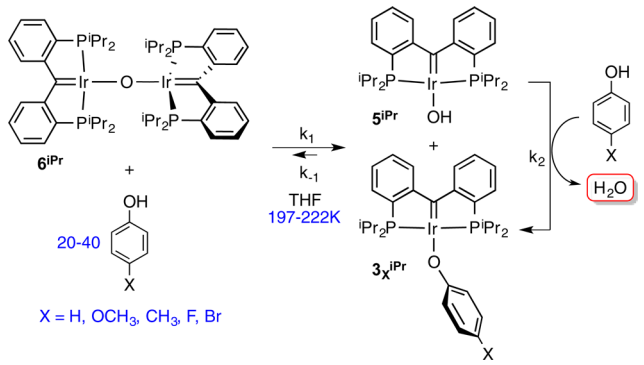

reactivity is observed for other phenols with varying substitution in the *para*-X position. These reactions are instantaneous at room temperature but proceed at convenient rates for following by NMR spectroscopy at temperatures in the 197–222 K range. Presumably, the reaction with the first equivalent of phenol yields a 1:1 mixture of $\mathbf{3_X}^{i\mathrm{Pr}}$ and $\mathbf{5}^{i\mathrm{Pr}}$, but the hydroxo compound is not observed in these reactions. Separate experiments show that the hydroxo compound reacts very rapidly with phenol to produce $\mathbf{3_X}^{i\mathrm{Pr}}$ and 1 equiv of water, even at low temperatures leading to the conclusion that, relative to k_1 (and k_{-1}), k_2 is very rapid. Thus, when monitoring the disappearance of $[\mathbf{6}^{i\mathrm{Pr}}]$ under pseudofirst-order conditions, where [phenol] is in large excess (20–40 equiv relative to $[\mathbf{6}^{i\mathrm{Pr}}]$), k_{obs} is equal to k_1. Note that, although 1 equiv of water is produced in this step, we have shown that reaction of $\mathbf{6}^{i\mathrm{Pr}}$ with H_2O at temperatures below 253 K is negligible (*vide supra*), and so this reaction can be assumed to have little effect on the observed kinetics.

When the reaction of $\mathbf{6}^{i\mathrm{Pr}}$ (5 mM) with 20 equiv of phenol was followed by ^{31}P NMR spectroscopy at 217 K, its disappearance over time (>5 half-lives) exhibited pseudofirst-order behavior in that plots of $\ln[\mathbf{6}^{i\mathrm{Pr}}]/[\mathbf{6}^{i\mathrm{Pr}}]_0$ were linear; half-order plots were nonlinear.[73] The rate of appearance of product $\mathbf{5}^{i\mathrm{Pr}}$ was twice that of the disappearance of $\mathbf{6}^{i\mathrm{Pr}}$ and also exhibited first-order behavior, confirming that $k_2 > k_1$. When varying amounts of phenol were employed (20–40 equiv) in the reaction at 217 K, a plot of lnk_{obs} vs ln[phenol] was linear (Figure S5), producing a slope of 0.86 ± 0.11, showing that the reaction is overall second order, first order in both $[\mathbf{6}^{i\mathrm{Pr}}]$ and [phenol]. Evaluation of the observed rate constant (k_1) at four temperatures (197, 207, 217, and 222 K) allowed for an Eyring analysis, the data for which are shown in Figure 3. Unfortunately, the temperature range

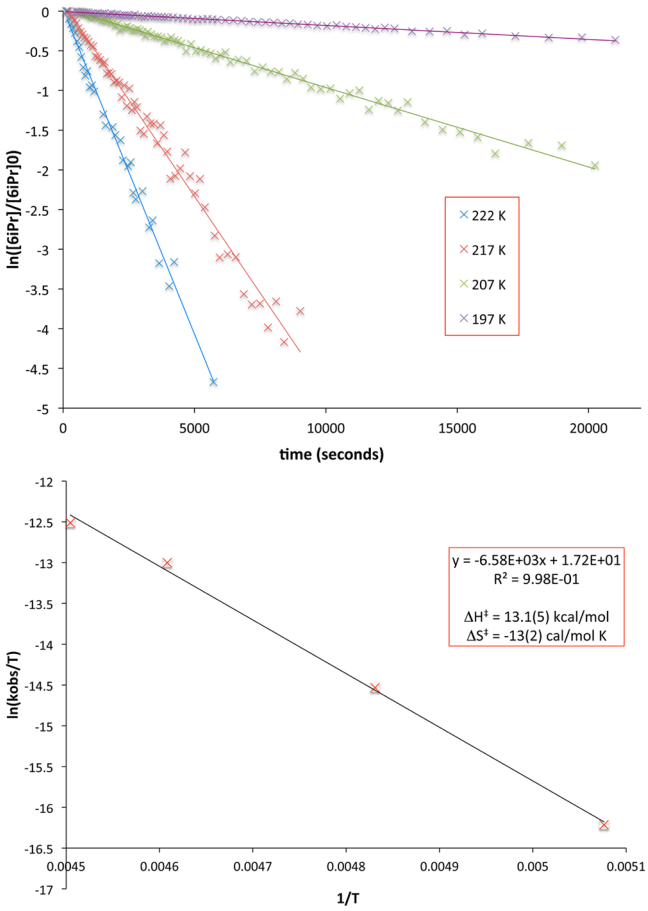

Figure 3. Top: Pseudofirst-order plots for the disappearance of $[\mathbf{6}^{i\mathrm{Pr}}]$ vs time at temperatures 197 (k_{obs} = 1.79(2) × 10^{-5} s^{-1}), 207 (k_{obs} = 1.0(1) × 10^{-4} s^{-1}), 217 (k_{obs} = 4.9(1) × 10^{-4} s^{-1}), and 222 (k_{obs} = 8.2(4) × 10^{-4} s^{-1}) K ($[\mathbf{6}^{i\mathrm{Pr}}]_0$ = 5 mM, THF, 20 equiv of phenol). Bottom: Eyring plot and activation parameters obtained.

we could conveniently access is quite narrow; nevertheless, the Eyring plot (Figure 3, bottom) exhibits good linearity. With this caveat in mind, the $\Delta S^{\ddagger}$ value of −13(3) cal mol^{-1} K^{-1} is consistent with a bimolecular rate-limiting step, while the $\Delta H^{\ddagger}$ value of 13.1(7) kcal mol^{-1} yields a relatively low free energy barrier, $\Delta G^{\ddagger}$, of 15.9(8) kcal mol^{-1} at 217 K.[74,75] A second caveat

dx.doi.org/10.1021/ja412650s | J. Am. Chem. Soc. 2014, 136, 3256−3263

in the interpretation of the data discussed above lies in the tendency of phenols to form H-bonded aggregates of ill-defined nuclearity in organic solvents.[76−78] This complex phenomenon is largely ignored in our reading of this data but may be related to the order in [phenol] manifesting as slightly lower than 1. Also, although $\Delta S^{\ddagger}$ is negative, the magnitude of this value is somewhat less negative than might be expected for a simple bimolecular reaction but perhaps consistent with deaggregation of phenol during the reaction.

In light of these caveats and the DFT analysis of $\mathbf{6}^{i\mathrm{Pr}}$ discussed above, two limiting scenarios in which a bimolecular reaction between the dinuclear μ-oxo complex and phenol (and by proxy, water) might be envisioned (Scheme 4). A HOMO directed path

Scheme 4

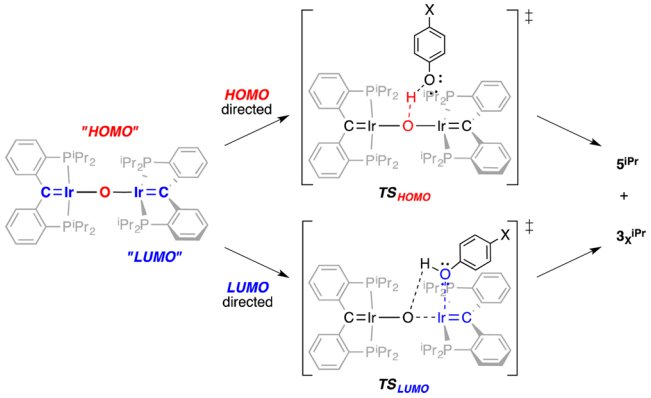

would involve deprotonation of the OH substrate by the bridging oxo group,[79,80] upon which a significant fraction of the two degenerate HOMO orbitals are localized. Here, the phenol approaches $\mathbf{6}^{i\mathrm{Pr}}$ such that O−H bond breakage dominates the transition state, leading directly to the hydroxo derivative $\mathbf{5}^{i\mathrm{Pr}}$ and perhaps the phenoxy compound $\mathbf{3}_{\mathrm{X}}^{i\mathrm{Pr}}$, although Ir−O bond formation may occur in a separate step. The other limiting path is a LUMO directed trajectory in which the phenol acts as a Lewis base toward one of the Ir centers, which contribute to some degree to the LUMO orbitals. In this scenario, phenoxy oxygen−iridium bond formation dominates the transition state, along with rupture of the Ir-μ-oxo bond.

Several observations point to a mechanism that has more "HOMO directed" character than "LUMO directed". First, in the coordination chemistry of $(PC_{sp^2}P)Ir(I)-X$ compounds, we have not observed any tendency to undergo reaction with Lewis bases, that is, coordination of ligands to the Ir center in a dative sense does not appear to be a prominent feature of their chemistry. This is consistent with the character of the degenerate LUMO pair, which is more ligand-based than metal-based (Figure 2). Although d^8 square planar complexes tend to undergo associative ligand substitution, the steric and electronic properties of $\mathbf{6}^{i\mathrm{Pr}}$ make coordination of phenol to the metal an unlikely path for the observed reaction. A second observation in favor of a HOMO directed path is the occurrence of a primary kinetic isotope effect in the reaction of $\mathbf{6}^{i\mathrm{Pr}}$ with DOPh under the same conditions as those established above. The k_{obs} measured at 217 K in the presence of 20 equiv of d_1-phenol was $2.58(3) \times 10^{-4}$ s^{-1}, yielding a k_H/k_D of 1.90(6), which is similar in magnitude to other effects observed in deprotonation of O−H functions.[81,82] Thus, phenolic O−H bond cleavage is important in the transition state of this reaction, as predicted for the HOMO directed path.

A third line of evidence is comprised in the rate trends observed for various *para*-substituted phenols. For the HOMO directed path, more acidic substrates (X more electron withdrawing) would be expected to exhibit faster rates, while in the LUMO dominated path, more Lewis basic substrates (X more electron donating) would react faster. In fact, we observe the former trend (Figure 4), in which a Hammett plot[83]

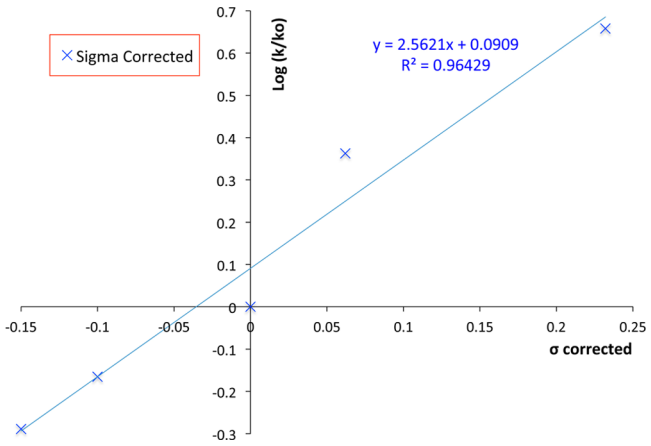

Figure 4. Hammett plot for the reactions of $\mathbf{6}^{i\mathrm{Pr}}$ with *para*-X-C_6H_4OH (X = F, Br, H, Me, OMe) under pseudofirst-order conditions at 217 K.

gives reasonable correlations of log k_X/k_H with σ_{corr} values, with positive ρ values of 2.6 (see also Table S2). Thus, reaction of $\mathbf{6}^{i\mathrm{Pr}}$ with *para*-methoxy phenol is an order of magnitude slower than the reaction with *para*-bromo phenol under the same conditions. In fact, the reaction of $\mathbf{6}^{i\mathrm{Pr}}$ with *para*-nitro phenol was too fast at 217 K to assess using our protocols. These observations are completely consistent with a rate-determining step that involves protonation of the μ-oxo ligand.

Assuming that the reaction proceeds with HOMO directed character via a TS_{HOMO} close to that depicted in Scheme 4, the path of descent to products from this transition state remains experimentally opaque based on our data. A concerted production of the product mixture is plausible if OR^- is delivered to an iridium center as protonation of the oxo ligand occurs. However, a stepwise process as depicted in Scheme 5 is also a

Scheme 5

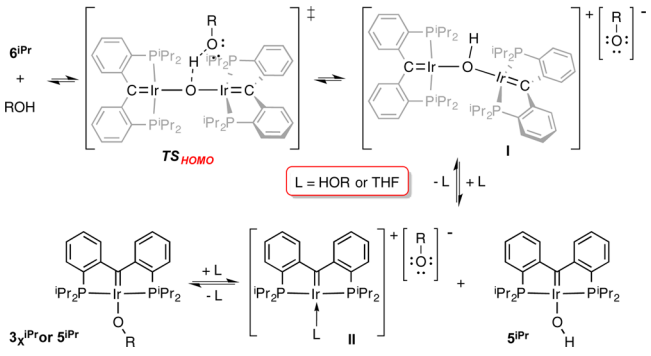

possibility. Here, the protonated oxo ion pair **I** rapidly dissociates to 1 equiv of observed hydroxo product $\mathbf{5}^{i\mathrm{Pr}}$ and the ligand stabilized cationic species **II**, paired with an $[OR]^-$ counteranion, which rapidly displaces L to form the other product—either a second equivalent of $\mathbf{5}^{i\mathrm{Pr}}$ or a phenoxide $\mathbf{3}_{\mathrm{X}}^{i\mathrm{Pr}}$. Cations **I** and **II** are

dx.doi.org/10.1021/ja412650s | J. Am. Chem. Soc. 2014, 136, 3256−3263

related in that, for **I**, L is the hydroxo complex **5**$^{i\mathrm{Pr}}$. These compounds have precedence in that they can be made with less reactive counteranions by halide abstraction from the chloride **2**$^{i\mathrm{Pr}}$ in the presence of a suitable L donor.[60] In the present chemistry, ion pairs **I** and **II** are stabilized by the polarity of the medium—water, ArOH and THF can all serve as ligands L—and the fact that the strongly donating carbene moiety of the $PC_{sp^2}P$ ligand labilizes the ligand that is coordinated in the *trans* position. This picture of the reaction implies that, by the principle of microscopic reversibility,[65] in forming the μ-oxo complex **6**$^{i\mathrm{Pr}}$ the first step involves ionization of **5**$^{i\mathrm{Pr}}$ by dissociation of $[OH]^-$, a process again aided by the strong donor properties of the anchoring carbene moiety in the $PC_{sp^2}P$ pincer ligand.

CONCLUSIONS

The condensation of 2 equiv of a terminal iridium hydroxo complex, **5**$^{i\mathrm{Pr}}$, to give the blue oxo bridged dinuclear species **6**$^{i\mathrm{Pr}}$ and water provides a well-defined system for study of the interconversion of these two archetypical oxygen-based ligands. The μ-oxo species in particular is notable, since most late metal oxo species tend to be in higher oxidation states.[84−86] Dinuclear **6**$^{i\mathrm{Pr}}$ is comprised of formally Ir(I) centers and is supported by an electron-rich ancillary $PC_{sp^2}P$ pincer ligand in which the central carbene is best described as a neutral donor.[60] As a consequence, the μ-oxo ligand is quite basic, and we propose that it reacts with ROH reagents via protonation of the oxo ligand. Unfortunately, controlled protonation of the oxo moiety using a Bronsted acid with a weakly coordinating ligand leads only to decomposition, so the presence of a strongly ligating conjugate base is necessary for clean reactions. Nonetheless, the highly reactive nature of these species provides a useful platform for the examination of the reactivity of oxygen-based ligands in coordination environments relevant to water activation processes and the potential for the rational generation of reactive intermediates. Studies along these lines utilizing the $PC_{sp^2}P$ ligand framework are continuing.

EXPERIMENTAL SECTION

General methods are described in detail in the Supporting Information.

Synthesis of bis-(2-(Di-*tert*-butylphosphino)phenyl) Methylidene Iridium Hydroxo, 5$^{t\mathrm{Bu}}$. To a flask charged with **2**$^{t\mathrm{Bu}}$ (0.050 g, 0.075 mmol), 3 mL of basified, filtered, cooled to −30 °C THF was added. In a separate vial, cesium hydroxide hydrate (0.020 g, 0.13 mmol) was suspended in 1 mL of the same THF and added dropwise to the flask. The solution was stirred for 5 min and then heated to 65 °C for 20 h. The solvent was removed *in vacuo*, and hexane was added to the resultant green residue. The solution was triturated for 15 min, the solvent was removed, and this procedure was carried out twice more. Hexane was added a fourth time, the solution was filtered through a frit, and the solvent was removed. The filtrate was isolated as a green solid in 92% yield. **5**$^{t\mathrm{Bu}}$-d_1 (OD) was prepared by successive addition of D_2O to **5**$^{t\mathrm{Bu}}$ and removal *in vacuo* and performed in triplicate. ^{1}H NMR (400 MHz, C_6D_6) δ: 8.09 (d, $^3J_{HH}$ = 8.0 Hz, 2H, C**H**, Ar), 7.83 (t, $^3J_{HH}$ = 7.4 Hz, 2H, C**H**, Ar), 7.45 (m, 2H, C**H**, Ar), 6.48 (t, $^3J_{HH}$ = 7.6 Hz, 2H, C**H**, Ar), 4.22 (t, $^3J_{HP}$ = 3.8 Hz, 1H, O**H**), 1.58 (vt, $^3J_{PH}$ = 6.7 Hz, 36H, C**H**$_3$, ^{t}Bu). ^{13}C{^{1}H} NMR (101 MHz, C_6D_6) δ: 202.7 (vt, $^2J_{CP}$ = 2.9 Hz, **C**=Ir), 179.1 (vt, $^2J_{CP}$ = 17.3 Hz, **C**−C-P, Ar), 137.1 (vt, $^1J_{CP}$ = 18.2 Hz, **C**-P, Ar), 136.3 (s, **C**H, Ar), 132.6 (s, **C**H, Ar), 125.2 (vt, $^3J_{CP}$ = 3.2 Hz, **C**H, Ar), 122.6 (vt, $^2J_{CP}$ = 6.8 Hz, **C**H, Ar), 36.1 (vt, $^1J_{CP}$ = 9.2 Hz, **C**(CH$_3$)$_3$, ^{t}Bu), 31.6 (vt, $^2J_{CP}$ = 3.4 Hz, **C**H$_3$, ^{t}Bu). ^{31}P{^{1}H} NMR (162 MHz, C_6D_6): δ 58 (s). IR (NaCl) cm^{-1}: ν_{OH} 3642 (m), ν_{OD} 2688 (m). HRMS (EI) calcd for $C_{29}H_{45}P_2IrO$ (M+) 664.2575, found: 664.2554. Elemental analysis calcd (%) for $C_{29}H_{45}P_2IrO$: C 52.47, H 6.83; found: C 53.72, H 6.50.

Synthesis of bis-(2-(Di-*iso*-propylphosphino)phenyl) Methylidene Iridium Hydroxo, 5$^{i\mathrm{Pr}}$. To a solution of **2**$^{i\mathrm{Pr}}$ (0.061 g, 0.097 mmol) in 3 mL THF cooled to −30 °C, a suspension of cesium hydroxide monohydrate (0.040 g, 0.23 mmol) in THF at −30 °C was added dropwise. The resulting deep green solution was allowed to warm slowly to room temperature and stirred under an argon atmosphere for 12 h. After 12 h, the solution was dull green in color. The solvent was removed *in vacuo*, and pentane was added. Filtration through a frit afforded a turquoise solution. One mL of degassed water was added to the pentane solution, giving a green solution, and stirred at room temperature for 1 h. The solvent was removed *in vacuo*, and the resulting semi-solid was pumped at room temperature for 1 h. The product was isolated in 70% yield as a dark green solid. **5**$^{i\mathrm{Pr}}$-d_1 (OD) was prepared by successive addition of D_2O to **5**$^{i\mathrm{Pr}}$ and removal *in vacuo*, performed in triplicate. ^{1}H NMR (400 MHz, C_6D_6): δ 8.11 (d, $^3J_{HH}$ = 7.8 Hz, 2H, C**H**, Ar), 7.81 (t, $^3J_{HH}$ = 7.2 Hz, 2H, C**H**, Ar), 7.03 (dt, $^3J_{HH}$ = 6.6, $^3J_{HP}$ = 2.9 Hz, 2H, C**H**, Ar), 6.50 (t, $^3J_{HH}$ = 7.5 Hz, 2H, C**H**, Ar), 4.31 (t, $^3J_{HP}$ = 3.8 Hz, 1H, O**H**), 2.77 (m, 4H, C**H**, ^{i}Pr), 1.43 (dvt, $^3J_{HH}$ = 15.4, $^3J_{HP}$ = 7.4 Hz, 12H, C**H**$_3$, ^{i}Pr), 1.23 (dvt, $^3J_{HP}$ = 7.0 Hz, 12H, C**H**$_3$, ^{i}Pr). ^{13}C{^{1}H} NMR (101 MHz, C_6D_6) δ: 204.8 (s, **C**=Ir), 178.3 (vt, $^2J_{CP}$ = 17.4 Hz, **C**−C-P, Ar), 137.7 (vt, $^1J_{CP}$ = 20.4 Hz, **C**-P, Ar), 134.8 (vt, $^3J_{CP}$ = 10.5 Hz, **C**H, Ar), 132.9 (vt, $^2J_{CP}$ = 10.8 Hz, **C**H, Ar), 125.6 (s, **C**H, Ar), 121.6 (vt, $^3J_{CP}$ = 6.7 Hz, **C**H, Ar), 24.8 (vt, $^1J_{CP}$ = 13.1 Hz, **C**H, ^{i}Pr), 20.3 (vt, $^2J_{CP}$ = 2.7 Hz, **C**H$_3$, ^{i}Pr), 19.5 (s, **C**H$_3$, ^{i}Pr). ^{31}P{^{1}H} NMR (162 MHz, C_6D_6): δ 45 (s). IR (NaCl plates) cm^{-1}: ν_{OH} 3625 (w), ν_{OD} 2685 (m). HRMS (ESI) calcd for $C_{25}H_{36}P_2IrO$ (M+) 607.1866, found 607.1841, HRMS (EI) calcd for $C_{25}H_{37}P_2IrO$ (M+) 608.1949, found 608.1924. Elemental analysis calcd (%) for $C_{25}H_{37}OP_2Ir$: C 49.41, H 6.14; found: C 49.98, H 6.35.

Synthesis of bis-[bis-(2-(Di-*iso*-propylphosphino)phenyl) Methylidene Iridium]-μ-oxo, 6$^{i\mathrm{Pr}}$. Water was removed from **5**$^{i\mathrm{Pr}}$ through heating of the solvent free solid to 80 °C for 12 h under dynamic vacuum. Attempts with 4 Å molecular sieves led to sufficient water removal, yet also decomposition due to the slightly acidic nature of molecular sieves. ^{1}H NMR (400 MHz, C_6D_6) δ 7.83 (d, $^3J_{HH}$ = 7.9 Hz, 2H, C**H**, Ar), 7.45 (t, $^3J_{HH}$ = 7.3 Hz, 2H, C**H**, Ar), 7.05 (dt, $^3J_{HH}$ = 6.7, $^3J_{HP}$ = 3.1 Hz, 2H, C**H**, Ar), 6.65 (t, $^3J_{HH}$ = 7.6 Hz, 2H, C**H**, Ar), 3.18 (m, 4H, C**H**, ^{i}Pr), 1.47 (dvt, $^3J_{HP}$ = 7.2 Hz, 12H, C**H**$_3$, ^{i}Pr), 1.39 (dvt, $^3J_{HP}$ = 6.9 Hz, 12H, C**H**$_3$, ^{i}Pr). ^{13}C{^{1}H} NMR (101 MHz, C_6D_6): δ 185.1 (s, **C**=Ir), 176.0 (vt, $^2J_{CP}$ = 16.8 Hz, **C**−C-P), 135.7 (vt, $^1J_{CP}$ = 21.9 Hz, **C**-P, Ar), 133.0 (s, **C**H, Ar), 131.9 (s, **C**H, Ar), 123.7 (s, **C**H, Ar), 121.3 (vt, $^2J_{CP}$ = 6.4 Hz, **C**H, Ar), 25.1 (vt, $^2J_{CP}$ = 12.0 Hz, **C**H, ^{i}Pr), 20.8 (s, **C**H$_3$, ^{i}Pr), 18.7 (s, **C**H$_3$, ^{i}Pr). ^{31}P{^{1}H} NMR (162 MHz, C_6D_6): δ 38 (s). IR (NaCl) cm^{-1}: ν_{OH} 3600 (w), ν_{OD} 2665 (w). Elemental analysis calcd (%) for $C_{50}H_{72}P_4Ir_2O$: C 50.15, H 6.06; found: C 50.48, H 6.41.

Kinetic Experiments. The series of experiments performed in order to obtain rate data for the conversion of **6**$^{i\mathrm{Pr}}$ to **3**$_X$$^{i\mathrm{Pr}}$ were low-temperature (217 ± 1 K) ^{31}P{^{1}H} NMR experiments (16 scans, d1 = 2.5 s) in d_8-THF using triphenylphosphine (0.057 M) as the internal standard. The ^{31}P{^{1}H} NMR T_1 relaxation of **6**$^{i\mathrm{Pr}}$ was 183 ms for a 30° pulse. Solutions of **6**$^{i\mathrm{Pr}}$ (0.0084 M in d_8-THF) were prepared each day of kinetic measurements to ensure minimal production of **5**$^{i\mathrm{Pr}}$. Phenol was sublimed and stored in the glovebox, where appropriate concentration solutions were prepared. A standard 5 mm NMR tube was charged with 0.35 mL of **6**$^{i\mathrm{Pr}}$ solution and 0.05 mL of triphenylphosphine solution (0.05 M) in the glovebox, while the phenol solution was sealed in a syringe (for 20 equiv, 0.11 mL, 0.53 M). The magnet was cooled to 217 K, and a control ^{31}P{^{1}H} NMR spectrum was recorded. A −78 °C dry ice/acetone bath was prepared, and the reaction mixture was cooled for 5 min. The phenol solution was then injected slowly as to form a layer. After an additional 5 min to ensure temperature consistency in both layers, the tube was shaken vigorously and inserted into the magnet (time = 0). Once lock was established, successive ^{31}P{^{1}H} NMR spectra were recorded over time, and the disappearance of **6**$^{i\mathrm{Pr}}$ was measured to obtain rate constants. While the corresponding iridium phenoxide complexes **3**$_X$$^{i\mathrm{Pr}}$ were not isolated, each was prepared quantitatively in an NMR tube reaction (0.010 g, 0.008 mmol **6**$^{i\mathrm{Pr}}$ and equimolar *p*-x-phenol in d_8-THF) and characterized fully by NMR spectroscopy; the characterization data for each complex (X = OMe, Me, F, Br) is provided in the Supporting Information.

dx.doi.org/10.1021/ja412650s | J. Am. Chem. Soc. 2014, 136, 3256−3263

■ ASSOCIATED CONTENT

Supporting Information

Crystallographic data files for 6^{iPr} (CCDC 976854) as well as relative energies and *x,y,z* coordinates of the calculated structures and the full list of authors for ref 62. This material is available free of charge via the Internet at http://pubs.acs.org.

■ AUTHOR INFORMATION

Corresponding Author

wpiers@ucalgary.ca

Notes

The authors declare no competing financial interest.

■ ACKNOWLEDGMENTS

Funding for the experimental work described was provided by the Natural Sciences and Engineering Research Council of Canada in the form of a Discovery Grant to W.E.P. D.H.E. thanks BYU and the Fulton Supercomputing Lab. W.E.P. thanks the Canada Council for the Arts for a Killam Research Fellowship (2012-2014). We thank an anonymous reviewer for raising the important issue of hydrogen-bonded phenol aggregates and their likely role in the chemistry described.

■ REFERENCES

(1) Hartwig, J. F. *Organotransition metal chemistry: from bonding to catalysis*; University Science Books: Sausalito, CA, 2010.
(2) Labinger, J. A.; Bercaw, J. E. *Nature* **2002**, *417*, 507−514.
(3) Trnka, T. M.; Grubbs, R. H. *Acc. Chem. Res.* **2000**, *34*, 18−29.
(4) Brintzinger, H. H.; Fischer, D.; Mülhaupt, R.; Rieger, B.; Waymouth, R. M. *Angew. Chem., Int. Ed. Engl.* **1995**, *34*, 1143−1170.
(5) Weinberg, D. R.; Gagliardi, C. J.; Hull, J. F.; Murphy, C. F.; Kent, C. A.; Westlake, B. C.; Paul, A.; Ess, D. H.; McCafferty, D. G.; Meyer, T. J. *Chem. Rev.* **2012**, *112*, 4016−4093.
(6) Rosenthal, J.; Nocera, D. G. *Acc. Chem. Res.* **2007**, *40*, 543−553.
(7) Decharin, N.; Popp, B. V.; Stahl, S. S. *J. Am. Chem. Soc.* **2011**, *133*, 13268−13271.
(8) Denney, M. C.; Smythe, N. A.; Cetto, K. L.; Kemp, R. A.; Goldberg, K. I. *J. Am. Chem. Soc.* **2006**, *128*, 2508−2509.
(9) Fulmer, G. R.; Muller, R. P.; Kemp, R. A.; Goldberg, K. I. *J. Am. Chem. Soc.* **2009**, *131*, 1346−1347.
(10) Lewis, N. S.; Nocera, D. G. *Proc. Natl. Acad. Sci. U.S.A.* **2006**, *103*, 15729−15735.
(11) Ozerov, O. V. *Chem. Soc. Rev.* **2009**, *38*, 83−88.
(12) Hull, J. F.; Balcells, D.; Blakemore, J. D.; Incarvito, C. D.; Eisenstein, O.; Brudvig, G. W.; Crabtree, R. H. *J. Am. Chem. Soc.* **2009**, *131*, 8730−8731.
(13) Lalrempuia, R.; McDaniel, N. D.; Müller-Bunz, H.; Bernhard, S.; Albrecht, M. *Angew. Chem., Int. Ed.* **2010**, *49*, 9765−9768.
(14) Blakemore, J. D.; Schley, N. D.; Balcells, D.; Hull, J. F.; Olack, G. W.; Incarvito, C. D.; Eisenstein, O.; Brudvig, G. W.; Crabtree, R. H. *J. Am. Chem. Soc.* **2010**, *132*, 16017−16029.
(15) Codolà, Z.; M. S. Cardoso, J.; Royo, B.; Costas, M.; Lloret-Fillol, J. *Chem.—Eur. J.* **2013**, *19*, 7203−7213.
(16) Savini, A.; Bellachioma, G.; Ciancaleoni, G.; Zuccaccia, C.; Zuccaccia, D.; Macchioni, A. *Chem. Commun.* **2010**, *46*, 9218−9219.
(17) McDaniel, N. D.; Coughlin, F. J.; Tinker, L. L.; Bernhard, S. *J. Am. Chem. Soc.* **2007**, *130*, 210−217.
(18) Bucci, A.; Savini, A.; Rocchigiani, L.; Zuccaccia, C.; Rizzato, S.; Albinati, A.; Llobet, A.; Macchioni, A. *Organometallics* **2012**, *31*, 8071−8074.
(19) Hetterscheid, D. G.; Reek, J. N. *Angew. Chem., Int. Ed. Engl.* **2012**, *51*, 9740−7.
(20) Grotjahn, D. B.; Brown, D. B.; Martin, J. K.; Marelius, D. C.; Abadjian, M.-C.; Tran, H. N.; Kalyuzhny, G.; Vecchio, K. S.; Specht, Z. G.; Cortes-Llamas, S. A.; Miranda-Soto, V.; van Niekerk, C.; Moore, C. E.; Rheingold, A. L. *J. Am. Chem. Soc.* **2011**, *133*, 19024−19027.
(21) Hintermair, U.; Hashmi, S. M.; Elimelech, M.; Crabtree, R. H. *J. Am. Chem. Soc.* **2012**, *134*, 9785−9795.
(22) Hintermair, U.; Sheehan, S. W.; Parent, A. R.; Ess, D. H.; Richens, D. T.; Vaccaro, P. H.; Brudvig, G. W.; Crabtree, R. H. *J. Am. Chem. Soc.* **2013**, *135*, 10837−10851.
(23) Graeupner, J.; Brewster, T. P.; Blakemore, J. D.; Schley, N. D.; Thomsen, J. M.; Brudvig, G. W.; Hazari, N.; Crabtree, R. H. *Organometallics* **2012**, *31*, 7158−7164.
(24) Turlington, C. R.; Harrison, D. P.; White, P. S.; Brookhart, M.; Templeton, J. L. *Inorg. Chem.* **2013**, *52*, 11351−11360.
(25) Brewster, T. P.; Blakemore, J. D.; Schley, N. D.; Incarvito, C. D.; Hazari, N.; Brudvig, G. W.; Crabtree, R. H. *Organometallics* **2011**, *30*, 965−973.
(26) Lohr, T. L.; Piers, W. E.; Parvez, M. *Inorg. Chem.* **2012**, *51*, 4900−4902.
(27) Kohl, S. W.; Weiner, L.; Schwartsburd, L.; Konstantinovski, L.; Shimon, L. J. W.; Ben-David, Y.; Iron, M. A.; Milstein, D. *Science* **2009**, *324*, 74−77.
(28) Poverenov, E.; Efremenko, I.; Frenkel, A. I.; Ben-David, Y.; Shimon, L. J. W.; Leitus, G.; Konstantinovski, L.; Martin, J. M. L.; Milstein, D. *Nature* **2008**, *455*, 1093−1096.
(29) Boisvert, L.; Goldberg, K. I. *Acc. Chem. Res.* **2012**, *45*, 899−910.
(30) Fulmer, G. R.; Herndon, A. N.; Kaminsky, W.; Kemp, R. A.; Goldberg, K. I. *J. Am. Chem. Soc.* **2011**, *133*, 17713−17726.
(31) Huacuja, R.; Graham, D. J.; Fafard, C. M.; Chen, C.-H.; Foxman, B. M.; Herbert, D. E.; Alliger, G.; Thomas, C. M.; Ozerov, O. V. *J. Am. Chem. Soc.* **2011**, *133*, 3820−3823.
(32) Betley, T. A.; Wu, Q.; Van Voorhis, T.; Nocera, D. G. *Inorg. Chem.* **2008**, *47*, 1849−1861.
(33) Sundstrom, E. J.; Yang, X.; Thoi, V. S.; Karunadasa, H. I.; Chang, C. J.; Long, J. R.; Head-Gordon, M. *J. Am. Chem. Soc.* **2012**, *134*, 5233−5242.
(34) Morales-Morales, D.; Lee, D. W.; Wang, Z.; Jensen, C. M. *Organometallics* **2001**, *20*, 1144−1147.
(35) Blum, O.; Milstein, D. *J. Am. Chem. Soc.* **2002**, *124*, 11456−11467.
(36) Yin, G. *Acc. Chem. Res.* **2012**, *46*, 483−492.
(37) Piers, W. E. *Organometallics* **2011**, *30*, 13−16.
(38) Burford, R. J.; Piers, W. E.; Parvez, M. *Organometallics* **2012**, *31*, 2949−2952.
(39) Weng, W.; Parkin, S.; Ozerov, O. V. *Organometallics* **2006**, *25*, 5345−5354.
(40) Weng, W.; Chen, C.-H.; Foxman, B. M.; Ozerov, O. V. *Organometallics* **2007**, *26*, 3315−3320.
(41) Gusev, D. G.; Lough, A. J. *Organometallics* **2002**, *21*, 2601−2603.
(42) Al-Salem, N. A.; Empsall, H. D.; Markham, R.; Shaw, B. L.; Weeks, B. *J. Chem. Soc., Dalton Trans.* **1979**, 1972−1982.
(43) Zhao, J.; Goldman, A. S.; Hartwig, J. F. *Science* **2005**, *307*, 1080−1082.
(44) Lesueur, W.; Solari, E.; Floriani, C.; Chiesi-Villa, A.; Rizzoli, C. *Inorg. Chem.* **1997**, *36*, 3354−3362.
(45) Boyd, L. M.; Clark, G. R.; Roper, W. R. *J. Organomet. Chem.* **1990**, *397*, 209−218.
(46) Hebden, T. J.; Goldberg, K. I.; Heinekey, D. M.; Zhang, X.; Emge, T. J.; Goldman, A. S.; Krogh-Jespersen, K. *Inorg. Chem.* **2010**, *49*, 1733−1742.
(47) Woerpel, K. A.; Bergman, R. G. *J. Am. Chem. Soc.* **1993**, *115*, 7888−7889.
(48) Ilg, K.; Werner, H. *Organometallics* **1999**, *18*, 5426−5428.
(49) Hetterscheid, D. G. H.; Reek, J. N. H. *Chem. Commun.* **2011**, *47*, 2712−2714.
(50) Sieh, D.; Schlimm, M.; Andernach, L.; Angersbach, F.; Nückel, S.; Schöffel, J.; Šušnjar, N.; Burger, P. *Eur. J. Inorg. Chem.* **2012**, *2012*, 444−462.
(51) Tahmassebi, S. K.; Conry, R. R.; Mayer, J. M. *J. Am. Chem. Soc.* **1993**, *115*, 7553−7554.
(52) Ladipo, F. T.; Kooti, M.; Merola, J. S. *Inorg. Chem.* **1993**, *32*, 1681−1688.

(53) Millard, M. D.; Moore, C. E.; Rheingold, A. L.; Figueroa, J. S. *J. Am. Chem. Soc.* **2010**, *132*, 8921−8923.
(54) Klaring, P.; Pahl, S.; Braun, T.; Penner, A. *Dalton Trans.* **2011**, *40*, 6785−6791.
(55) Ritter, J. C. M.; Bergman, R. G. *J. Am. Chem. Soc.* **1997**, *119*, 2580−2581.
(56) Meier, S. K.; Young, K. J. H.; Ess, D. H.; Tenn, W. J.; Oxgaard, J.; Goddard, W. A.; Periana, R. A. *Organometallics* **2009**, *28*, 5293−5304.
(57) Miller, C. A.; Janik, T. S.; Lake, C. H.; Toomey, L. M.; Churchill, M. R.; Atwood, J. D. *Organometallics* **1994**, *13*, 5080−5087.
(58) Green, L. M.; Meek, D. W. *Organometallics* **1989**, *8*, 659−666.
(59) Ortmann, D. A.; Werner, H. *Z. Anorg. Allg. Chem.* **2002**, *628*, 1373−1376.
(60) Burford, R. J.; Piers, W. E.; Parvez, M. *Eur. J. Inorg. Chem.* **2013**, 3826−3830.
(61) Fortner, K. C.; Laitar, D. S.; Muldoon, J.; Pu, L.; Braun-Sand, S. B.; Wiest, O.; Brown, S. N. *J. Am. Chem. Soc.* **2006**, *129*, 588−600.
(62) Frisch, M. J. et al. *Gaussian 09*, revision B.01; Gaussian Inc.: Wallingford, CT, 2009. See SI for full citation.
(63) Zhao, Y.; Truhlar, D. G. *Theor. Chem. Acc.* **2008**, *120*, 215.
(64) Zhao, Y.; Truhlar, D. G. *Acc. Chem. Res.* **2008**, *41*, 157−167.
(65) Burwell, R. L.; Pearson, R. G. *J. Phys. Chem.* **1966**, *70*, 300−302.
(66) Mak, T. C. W.; McMullan, R. K. *J. Chem. Phys.* **1965**, *42*, 2732−2737.
(67) Jones, C. Y.; Zhang, J. S.; Lee, J. W. *Journal of Thermodynamics* **2010**, *2010*, article ID 583041.
(68) Melnick, J. G.; Radosevich, A. T.; Villagran, D.; Nocera, D. G. *Chem. Commun.* **2010**, *46*, 79−81.
(69) Morales-Morales, D.; Redón, R.; Wang, Z.; Lee, D. W.; Yung, C.; Magnuson, K.; Jensen, C. M. *Can. J. Chem.* **2001**, *79*, 823−829.
(70) Kloek, S. M.; Heinekey, D. M.; Goldberg, K. I. *Organometallics* **2006**, *25*, 3007−3011.
(71) Ilg, K.; Werner, H. *Organometallics* **2001**, *20*, 3782−3794.
(72) Burford, R. J.; Piers, W. E., unpublished results.
(73) The rates of reactant disappearance/product disappearance were monitored through integration against a triphenylphosphine internal standard. No reaction between this phosphine and either reactant or product was observed, and rates were statistically identical in the absence of this standard, confirming its inert nature in this chemistry.
(74) Errors in the thermodynamic parameters were evaluated according to the method described in ref 75.
(75) Morse, P. M.; Spencer, M. D.; Wilson, S. R.; Girolami, G. S. *Organometallics* **1994**, *13*, 1646−1655.
(76) Kuhn, L. P. *J. Am. Chem. Soc.* **1952**, *74*, 2492−2499.
(77) Johnson, J. R.; Christian, S. D.; Affsprung, H. E. *J. Chem. Soc. (Resumed)* **1965**, 1−6.
(78) Tucker, E. E.; Christian, S. D.; Lin, L.-N. *J. Phys. Chem.* **1974**, *78*, 1443−1445.
(79) MacLeod, K. C.; Patrick, B. O.; Smith, K. M. *Inorg. Chem.* **2011**, *51*, 688−700.
(80) Pinkas, J.; Císařová, I.; Gyepes, R.; Kubišta, J.; Horáček, M.; Mach, K. *Organometallics* **2013**, *32*, 6306−6314.
(81) Kuss-Petermann, M.; Wolf, H.; Stalke, D.; Wenger, O. S. *J. Am. Chem. Soc.* **2012**, *134*, 12844−12854.
(82) Nishida, Y.; Morimoto, Y.; Lee, Y.-M.; Nam, W.; Fukuzumi, S. *Inorg. Chem.* **2013**, *52*, 3094−3101.
(83) Johnson, C. D. *The Hammett Equation*; Cambridge University Press: Cambridge, 1973.
(84) Cotton, F. A.; Lahuerta, P.; Sanau, M.; Schwotzer, W. *J. Am. Chem. Soc.* **1985**, *107*, 8284−8285.
(85) Dobbs, D. A.; Bergman, R. G. *J. Am. Chem. Soc.* **1993**, *115*, 3836−3837.
(86) Schau-Magnussen, M.; Malcho, P.; Herbst, K.; Brorson, M.; Bendix, J. *Dalton Trans.* **2011**, *40*, 4212−4216.

NOTE ADDED IN PROOF

Additional examples of Ir(I) hydroxo compounds have appeared in the recent literature: Nelson, D. J.; Truscott, B. J.; Slawin, A. M. Z.; Nolan, S. P., *Inorg. Chem.* **2013**, *52*, 12674−12681; Truscott, B. J.; Nelson, D. J.; Lujan, C.; Slawin, A. M. Z.; Nolan, S. P., *Chem. Eur. J.* **2013**, *19*, 7904−7916; Truscott, B. J.; Nelson, D. J.; Slawin, A. M. Z.; Nolan, S. P., *Chem. Commun.* **2014**, *50*, 286−288.